Near-surface geophysical mapping of an Upper Cretaceous submarine volcanic vent in Austin, Texas, USA

Mustafa Saribudak[1]

Abstract

Geophysical surveys were conducted at the Williamson Creek site south of Austin, Texas, to determine the structural relation of the Upper Cretaceous volcanic rocks (lava and tuff) with the associated Austin Chalk limestone. At this site, resistivity and magnetic methods were performed over the exposed volcanic and limestone rocks. Geophysical results indicate an excellent correlation between high-magnetic and low-resistivity anomalies. The pseudo-3D resistivity data show a steeply dipping funnel-shaped vent formation over the high-magnetic anomaly (up to 3000 nT). Magnetic anomalies are consistent with a uniformly magnetized body, like a volcanic vent, and the anomaly's dimensions are consistent with eroded volcanic vents in other distributed volcanic fields in the United States. Magnetic data has been integrated with resistivity data and geologic observations and subjected to 2.5D forward potential-field modeling. Modeling has revealed a perfect fit with three magnetic zones: (1) the central part corresponds to the main magma feeder (vent); (2) the surrounding zone corresponds to undifferentiated interbedded tuffs and lavas; and (3) the low-magnetization zone. Geophysical results show that additional resistivity surveys, in conjunction with magnetic surveys, could offer useful information on the shallow volcanic plugs (serpentines), which are potential oil and gas traps in Texas, and their adjacent sedimentary rocks. The procedures developed here may have applications in other areas with comparable geologic conditions.

Introduction

Geophysical methods, mostly gravity and magnetics, have been used across the world to better understand the internal structure of volcanic centers and the nature of the volcanic products (López Loera et al., 2008; Mrlina et al., 2009; Skácelová et al., 2010; Blaikie et al., 2012; Blaikie et al., 2014; George et al., 2015; Marshall et al., 2015). Points gathered from these papers, pertinent to this study, are: (1) magnetic anomalies generally are associated with near-vent facies and the structure of the upper parts of conduits in distributed volcanic fields; (2) magnetic anomalies associated with these structures are commonly on the order of 1000s nT; (3) use of geophysical surveys and applications of potential-field modeling are particularly important when vents are covered by sedimentation or obscured by erosion (e.g., Mrlina et al., 2009; Skácelová et al., 2010; George et al., 2015) and to determine the sizes of crater areas, especially where these are obscured by surface geology or cultural features (e.g., McLean and Betts, 2003; Blaikie et al., 2014; Marshall et al., 2015).

Electrical resistivity and electromagnetic surveys have been used for many decades in hydrogeologic, geotechnical, and environmental investigations (Griffiths and Turnbull, 1985; Dahlin, 1996; Dahlin and Loke, 1997; Connor and Sandberg, 2001; Dobecki and Church 2006; Saribudak et al., 2013). Resistivity surveys, however, have been used sporadically to explore the volcanic geology (Xia et al., 2010; De Filippis et al., 2013).

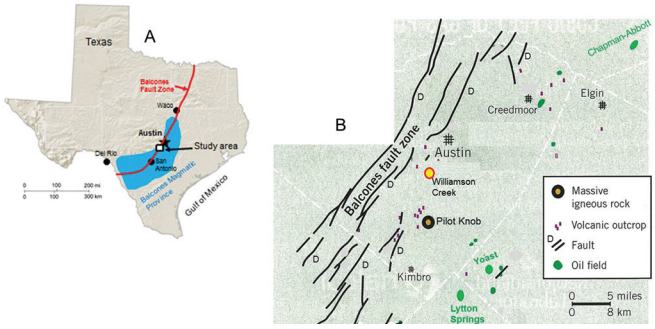

Figure 1. Maps showing (a) the Balcones Magmatic Province and the Balcones Fault Zone and (b) the Williamson Creek site (modified from Saribudak and Caran [2015]). Pilot Knob is one of the eroded cores of an extinct volcano located south of Austin.

In this study, a volcano-sedimentary section was mapped at the Williamson Creek site. At Williamson Creek, both resistivity and magnetic methods were used. The purpose of these geophysical surveys was to identify the geologic nature and structure of these volcanic rocks with their associated Austin Chalk limestone (Young et al., 1982; Young and Woodruff, 1985). Geophysical methods used in this study were selected because a large contrast in magnetization and electrical resistivity is expected between the volcanic rocks and the surrounding limestone. Significantly, this study adds another perspective in using the tuff mounds to infer oil traps, which has not been part of the volcanic literature so far (Saribudak and Caran, 2015).

Volcanic activity and geologic background

The variety of Late Cretaceous volcanic rocks exposed in the Austin area and elsewhere in the Balcones Magmatic Province (BMP) results from the interplay between submarine volcanic eruption and erosive sedimentary processes associated with submarine tuff complexes during the Upper Cretaceous time (Ewing and Caran, 1982; Griffin et al., 2005). Within this province, there are 200 occurrences of igneous rocks emplaced during the deposition of the Austin Chalk, aligned along strike-oriented regional faults and fractures of the Balcones faults of Miocene age and pre-Tertiary Balcones faults in Central Texas (Ewing and Caran, 1982; Figure 1). These igneous bodies consist of shallow igneous structures associated with vents and pyroclastic rocks and lavas erupted on the seafloor.

As a product of the eruptions, tuff mounds were formed by the hydration of basaltic glass over eruption centers (Ewing and Caran, 1982). After eruption, the mounds of pyroclastic material that accumulated around and over the volcanic centers underwent alteration by palagonitization, the hydration of basaltic glass. Tuff mounds in central Texas can rise to 50–100 m above the seafloor. A schematic model of an erupting submarine volcano through a

[1]Environmental Geophysics Associates.

http://dx.doi.org/10.1190/tle35110936.1.

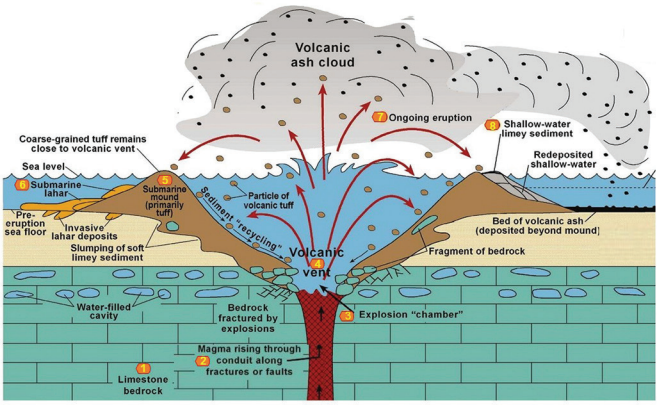

Figure 2. Schematic model of an erupting submarine volcano (modified from Caran et al. [2012] and Ewing and Caran [1982]). The construction of a tuff mound began with a "phreato magmatic" (steam + magma) eruption. Magma rising along a dike feeder met abundant water either at the seafloor or in a porous, water-saturated unit at moderate depth beneath the seafloor (Ewing and Caran [1982] and Caran et al. [2012]).

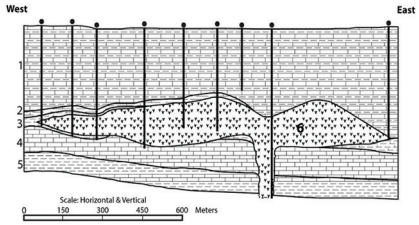

Figure 3. (Taken from Sellards [1932] and modified for simplicity.) West-east cross section of Chapman oil field showing relation of serpentine mass to overlying and underlying formations. (1) Taylor and overlying younger formations; (2) Taylor; (3) chalk stratum near base of Taylor; (4) Austin Chalk; (6) serpentine. Locations of nine oil wells (black dots) are shown along the cross section, seven of which are in the serpentine plug. The width of the eruption center is about 60 m.

vent or crater and formation of tuff mounds is shown in Figure 2. All of the known craters have been filled with tuff that slumped into the crater from the ring or accumulated during smaller, later-stage eruptions (Ewing and Caran, 1982).

Since Udden and Bybe (1916) first described them, significant hydrocarbon traps in and around tuff mounds are called "serpentine" or "volcanic" plugs (Ewing and Caran, 1982). Figure 1b shows some of the outcrops of the volcanic rocks and related oil fields, which occur along the Balcones Fault Zone in central Texas. One of these oil fields, called Chapman-Abbott, is located in the southeast corner of Williamson County, Texas, north of Austin (Figure 1b). Sellards (1932) illustrates the relationship of "serpentine plugs" and their structural and stratigraphic settings with respect to underlying and overlying sedimentary rocks along a west-east cross section of Chapman oil field (Figure 3). The cross section is about 1.5 km in length, and there are nine producing oil wells from the volcanic plug and associated sediments. The volcanic vent's width is about 60 m, and the thickness of the serpentine plug varies between 0 and 137 m. Ground-level magnetic surveys led directly to the discovery of similar oil fields, such as Hilbig, Jim Smith, Yoast, and Cedar Creek in the northern subprovince of Texas (Collingwood, 1930; Matthews, 1986).

The Late Cretaceous igneous rocks of the Balcones Magmatic Province (BMP) are highly silica-undersaturated; in order of relative abundance the observed rock types include: mellite-olivine nepheline basanite (50%), olivine nephelenite (30%), phonolite (10%), and alkali basalt (<5%) (Spencer, 1969). Burke et al. (1969) reported a K-Ar whole-rock age of 67.5 +/- 1.5 Ma. Much more precise dating (U-Pb and 40Ar/39Ar) of the igneous rocks for BMP indicates that the igneous activity occurred in two discrete phases: older mafic volcanism occurred between 81.5 and 84.1 Ma, and younger felsic volcanism between 76.2 and 78.8 Ma (Griffin et al., 2010).

Table 1. Stratigraphic relationship within the Austin Group (modified from Young and Woodruff, 1985). Underlying and overlying the Austin Group are Eagle Ford and Taylor Formations, respectively.

Formation	Description	Austin area (m)
Sprinkle	Massive, calcareous claystone	100
Pflugerville	Marly and chalky limestone	22
Burditt	Burditt Marl is a soft, clayey limestone	5
Dessau	Chalky limestone; dominantly a sparse to fairly dense limestone	25–30
Jonah	Thick beds of limestone; less chalky than Vinson	8
Vinson Chalk	Chalky limestone; contains soft and hard chalk; bottom contact with Atco is gradual	30
Atco	Alternating beds of massive limestone with more fissile limestone; contains much less chalk than Vinson Chalk	15–20

The Austin Chalk Group lies within the Balcones Fault Zone and outcrops in the Austin area. Young and Woodruff (1985) categorized the Austin Chalk Group into seven formations, identified in ascending order as: Atco, Vinson, Jonah, Dessau, Burditt, Pflugerville, and Sprinkle (Table 1).

Williamson Creek site

The volcanic section (tuff and lava) along the Williamson Creek site outcrops along Williamson Creek off of Emerald Forest Drive (Figures 1 and 4). This section is interpreted to be faulted against limestone of the Austin Group at either end (Ewing and Caran, 1982). The limestone is identified as the Vinson Chalk by Young et al. (1982). Western and eastern faults strike about N20E and dip 75° to the east and west, respectively, creating a graben-like structure (Ewing and Caran, 1982). The Vinson Chalk is about 30 m thick in the Austin area (Young and Woodruff, 1985; see Table 1).

On the creek bed, in addition to tuff and lava, there are volcaniclastic conglomerates, which consist of generally thick, indistinctly bedded packages of angular lapilli (up to 2 cm in diameter) and round to subrounded blocks of limestone (Caran et al., 2012). The lavas and associated deposits are generally heavily veined by calcite veins. Despite the alteration and jointing, the lavas are interpreted as relict pillows (Figures 5a and 5b).

Young et al. (1982) reported coarse-grained volcanic rocks to the north and south of this location. The volcanic rocks represented explosive volcanism based on petrologic evidence. Unfortunately,

urbanization has covered these outcrops now. Young et al. (1982) noted the presence of Dessau fossils in these volcaniclastic rocks and described them as being in stratigraphic contact with the Vinson Chalk. They interpreted this as evidence that the volcaniclastic rocks were deposited in an explosive crater that was excavated through the Dessau and Jonah Formation into the Vinson Chalk.

Figure 4. View of Vinson limestone juxtaposed to volcanic rocks (tuff and lava) at the Williamson Creek site. The contact, shown with a yellow line, dips toward the east at ~75º. This outcrop was exposed after a series of flooding during the early 2000s. The tuff (brownish color) appears to overlie the lava (pinkish color). The exposed length of the lava unit is about 10 m.

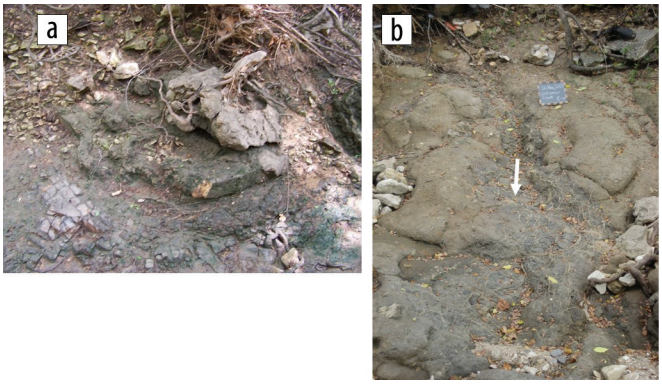

Figure 5. (a) Pillow lava and (b) lava tube structure on the bed of Williamson Creek. The arrow in 5b shows the direction of lava flow. (Photos courtesy of Alan Cherepon and Chris Caran, respectively).

Geophysical surveys and field-survey design

Five magnetic and nine resistivity profiles were surveyed across the volcanic section of Williamson Creek (Figure 6).

Magnetic method. A Geometrics G-858 Cesium magnetometer was used in the collection of the data. It measures the total earth's magnetic field rather than its vector components. Nanotesla (nT) is the unit of measure for the magnetometer. The collection rate of the magnetic data was 10 Hz, which corresponds to a data point less than a 0.3 m along the magnetic profiles.

The magnetic data were collected on two different dates. First, two baselines on the east and west of the study area were established, which were separated by about 160 m. Four profiles (M1 through M4) with a mixed profile spacing of 9, 12, and 9 m were surveyed perpendicular to these baselines (Figure 6). The data points along the profiles were converted to distances using Geometrics Magmap software (version 5.02). Varying, instead of fixed, profile spacing was due to site conditions, two small water ponds on the creek bed, and dense bushes and trees on the creek banks. A few months later on the second stage, an additional magnetic profile (MR) was run in order to explore the subsurface deeper with the resistivity. The length of profile MR was 201 m. The spatial accuracy of the surveys was about +/- 1 m.

A base station was established in the site's vicinity to record daily variations of the earth's magnetic field. The magnetic survey time during both stages was less than a half hour, and there were no significant diurnal variations. For this reason, a diurnal correction was not applied to the magnetic data. The background magnetic value for the site was 47,400 nT.

Prior to the magnetic surveys, all metallic and other types of garbage were picked up in order to collect good-quality data. The raw magnetic data were smoothed out by using a low-pass filter with a 6 m cutoff wavelength. Processing and modeling of the magnetic data were done with Geosoft Oasis Montaj software (version 7.2).

Resistivity method. The 2D resistivity method images the subsurface by applying a constant current in the ground through two current electrodes and measuring the resulting voltage differences at two potential electrodes some distance away. An apparent resistivity value is the product of the measured resistance and a geometric correction for a given electrode array. Resistivity values (ohm-m) are highly affected by several variables, including the presence of water or moisture, the amount and distribution of pore space in the material, and temperature.

Advanced Geosciences Inc. (AGI) SuperSting R1 and R8 resistivity meters were used with a mixed dipole-dipole and inverse Schlumberger electrode array. This array is sensitive to horizontal and vertical changes in the subsurface (compared to other arrays) and, when the data is inverted, provides a 2D electrical image

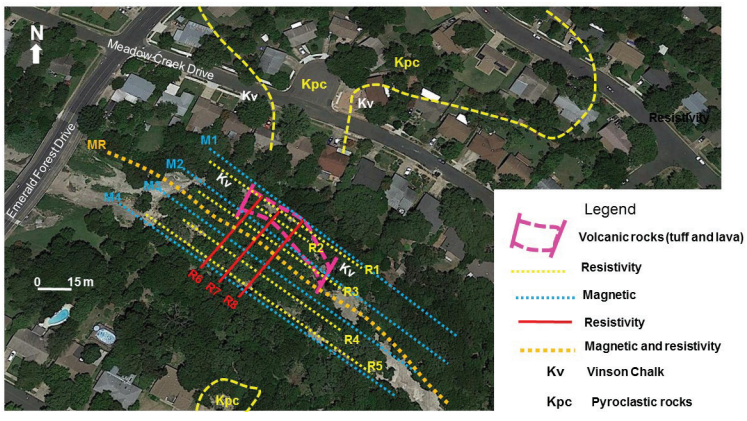

Figure 6. Map showing locations of Williamson Creek, geophysical profiles, and outcrops of the Austin Chalk and volcanic rocks. Dashed yellow lines indicate the boundaries of volcanic pyroclastic rocks mapped by Young et al. (1982). These outcrops are no longer visible due to urbanization. The width of the exposed volcanic section is about 50 m. Latitude and longitude of the site where the volcanic section is exposed are about 30º 21´ 55" and 97º 78´ 70".

of the near-surface geology. AGI's 2D and 3D Earth Imager software were used to process the resistivity data.

Six northwest-southeast and three northeast-southwest resistivity profiles were surveyed, with varying electrode spacing, along the Williamson Creek site (Figure 6). Profile R1 was located on the creek's northern bank. Profile M2 was placed on the creek bed. The rest of the profiles (R3, R4, and R5) were located on the southern creek bank (Figure 4). Profile MR is the longest profile, lengthwise. Northwest-southeast profiles are taken across the creek bed and are shown with labels R6, R7, and R8. The profile spacing was 6 m, and length was 41 m, respectively.

Interpretation of geophysical results at Williamson Creek site

Magnetic data. Filtered magnetic data, taken along four profiles (M1, M2, M3, and M4), are shown together in Figure 7. The y axis of each profile was fixed between the same ranges of magnetic values (46,500 nT for minimum and 51,500 nT for maximum) so that a comparison between profiles can be made. Two arrows on profiles M1 and M2 indicate the vertical contacts of the volcanic rocks against the Vinson Chalk that were observed in the field. Both profiles show up to 51,000 nT amplitude over the width of 50 m of volcanic rocks. The source of the steep gradient on profile M1, in the vicinity of the northwest contact, is not known, but it could be due to briefly unstable magnetometer positioning due to the steep, wet rock surfaces.

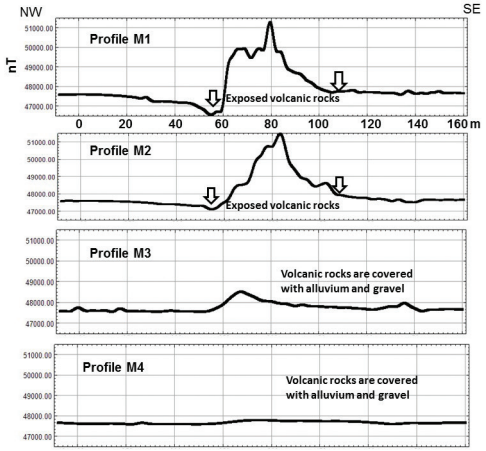

Figure 7. Four northwest-southeast magnetic profiles (M1 through M4) collected across the volcanic and limestone rocks at the Williamson Creek site (see Figure 6 for location). The width of the magnetic anomaly on profile M1 and M2 is about 50 m, and it fades away farther south along profiles M3 and M4.

Profile M3 provides a similar anomaly pattern to both M1 and M2, but the highest amplitude observed on M3 is 48,500 nT, dropping about 1500 nT from two previous profiles (Figure 7). Profile M4 indicates a rather broader anomaly, and its highest amplitude is about 47,800 nT, dropping about 700 nT from profile M3.

The background magnetic value at the study area is about 47,400 nT. Amplitudes of 48,500 to 51,000 nT magnetic values observed on profiles M1, M2, and M3 are consistent with a uniformly magnetized body, like a volcanic plug. However, the magnetic amplitude on profile M4 drops sharply to 47,800 nT. This reduction in magnetic intensity could be caused by either increased depth of the volcanic rocks and/or a change in magnetic susceptibility. The magnetic profile MR (see Figure 6 for location) will be discussed together with the resistivity data in the next section. The magnetic data observed on four profiles do not suggest a fault-like anomaly on either side of the volcanic outcrop.

Northwest-southeast resistivity data. Figure 8 shows the resistivity data collected along profiles R1, R2, and R3. Highest and lowest resistivity values along five northwest-southeast profiles are fixed as 300 to 10 Ω.m (except R2), respectively, so that there is a consistency between the profiles. The R2 profile was surveyed on the creek bed, and the weathered rocks had much lower resistivity values with respect to other profiles. The beginning of the horizontal distance for each profile also was adjusted with respect to profile R1.

The resistivity data along profile R1 indicates a sharp contact between the observed Vinson chalk and the volcanic rocks at station 37 m in the northwestern section; however, it does not show any change in resistivity values across the southeastern fault. This is probably due to 1 m thick alluvium cover in the eastern section. Volcanic rocks appear to have resistivity values ranging between 10 and 30 Ω.m (indicated in blue in Figure 8). Note that the volcanic deposits sit horizontally on the underlying limestone layers in the eastern section of the resistivity profile, which have resistivity values varying between 40 and 200 Ω.m. This uniformity, however, is broken due to the chaotic distribution of high- (limestone) and low- (volcanic) resistivity values in the vicinity of the western termination of the volcanic rocks.

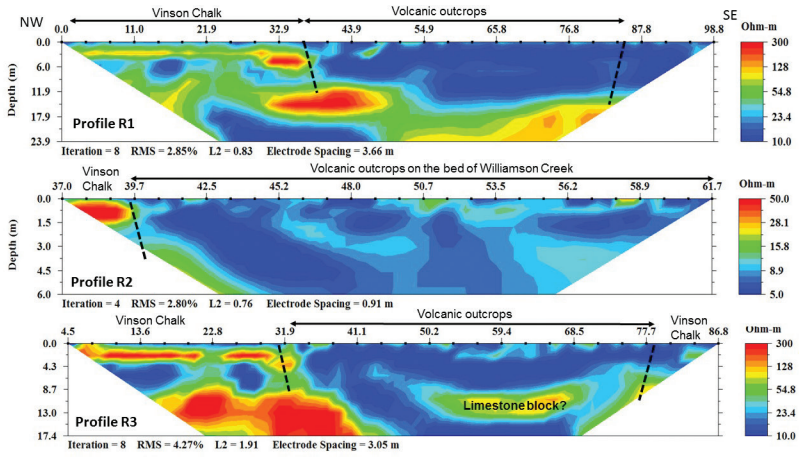

Figure 8. Resistivity data taken along profiles R1, R2, and R3. Dashed-black lines on the resistivity section correspond precisely to the geologic contacts observed in the field. Magnetic profiles M1 and M2 are approximately aligned with resistivity profiles R1 and R3 and show an amplitude of 51,000 nT across the volcanic rocks where low-resistivity values are observed. The observed contacts between the volcanic section and the Vinson Chalk, and its dipping direction, are shown with a dashed black line.

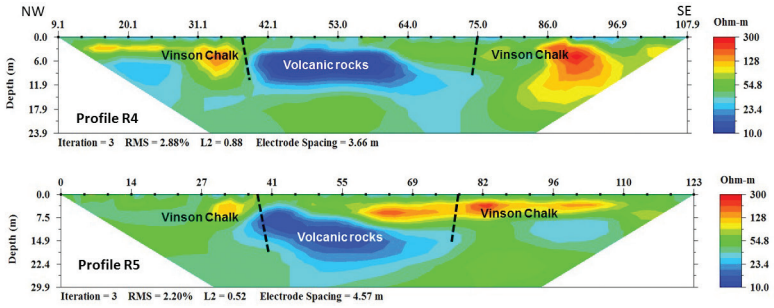

Figure 9. Resistivity data along profiles R4 and R5 on the southern bank of Williamson Creek. Geologic contacts (dashed black lines) observed on the bed of the creek extended and projected on the resistivity data. High magnetic values on profiles M3 and M4 (~48,500 and 47800 nT, respectively), which are located near these resistivity profiles, correspond to the low-resistivity anomalies, as depicted with the blue color.

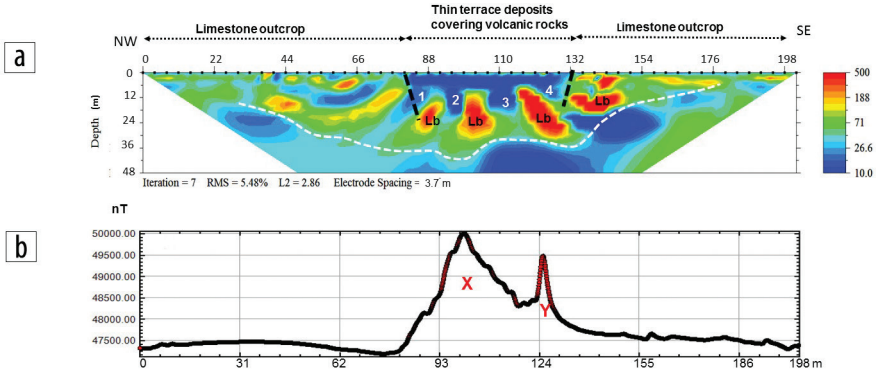

Figure 10. (a) Resistivity and (b) magnetic data along profile MR on the south bank of Williamson Creek. High resistive, fragmented limestone blocks (Lb) underlie the low-resistive volcanic rocks. Note the interfingering geometry of the volcanic rocks, shown with numbers 1, 2, 3, and 4. Locations of contacts (dashed-black lines) are precisely shown on the resistivity map because they were observable on the bed of the creek. The width of the volcanic section is approximately 50 m. The magnetic data indicates two high anomalies, shown with letters X and Y.

Profile R2 shows the resistivity data taken on the bed of the creek. Profile R2 starts on the Vinson Chalk and terminates in the volcanic rocks, which consist of volcanic tuff and lavas (see also Figure 2) This profile is short in length (25 m) because of the presence of creek water ponded on both sides of the profile. Volcanic rocks have resistivity values varying between 3 and 50 Ω.m. The western contact between the volcanic conglomerate and limestone and its dipping direction are shown with a dashed-black line.

Profile R3 is located immediately on the southern bank of Williamson Creek (Figure 8). The volcanic rocks are indicated by resistivity values ranging between 10 and 30 Ω.m (indicated in blue). Locations of the geologically interpreted faults (Caran et al., 2012) are superimposed by thick black dashed lines on the resistivity section. The northwestern geologic contact is well indicated by the resistivity data at station 30 m. The resistivity data on the southeast section do not show any visible contact between volcanic and limestone rocks. The volcanic rocks appear to envelope a relatively higher resistivity block (40 to 200 Ω.m) between stations 46 and 64 m at a depth of 11 m.

The resistivity data along profiles R4 and R5 are given in Figure 9. There is a well-defined low-resistivity anomaly located between stations 40 and 64 m (indicated in blue). Geologic contacts observed in the creek are covered here with alluvium and gravels. Thus, the azimuths of these contacts are projected onto these profiles, and they appear to correlate well with the geometry of the low-resistivity anomaly. The resistivity of this source ranges between 10 and 30 Ω.m, which correlates well with the known resistivity values of volcanic rocks observed along Williamson Creek. This anomaly is about 9 m thick and appears to be flat and slightly southeast dipping within more resistive rocks of Vinson limestone.

Profile R5 displays a well-defined low-resistivity anomaly between stations 38 and 73 m, as observed along profile R4. The resistivity anomaly ranges between 10 and 30 Ω.m, which correlates well with the known resistivity values of the volcanic rocks observed along Williamson Creek. The anomaly dips about 20° toward the east, and its thickness varies from 8 to 16 m. The bottom layer of the low-resistivity anomaly appears to reach to a depth of 27 m.

Resistivity and magnetic data collected along profile MR are shown in Figures 10a and 10b. The length of this profile is 201 m, which yields to a maximum exploration depth of 48 m in the central section of the resistivity data. Geologic contacts, which are based on the field observation, are shown on the resistivity profile as thick, black dashed lines (Figure 10a).

The resistivity data indicates a chaotic structure beneath the volcanic and limestone layers. The uniform structure of the volcanic rocks observed in the field and resistivity profiles R4 and R5 change dramatically at a depth of 11 m. The bottom layers of volcanic rocks indicate an irregular paleotopography, which interfinger into the depths of higher resistive units at four locations, numbered on the resistivity profile as 1, 2, 3, and 4 (Figure 10a). Large, randomly distributed resistive blocks, which have resistivity values up to 500 Ω.m, are located beneath the bottom layers of volcanic rocks. The high-resistive bodies could be limestone blocks, labeled on the resistivity section as Lb, and they appear to be contained within a geologic unit that has a resistivity variation between 40 and 100 Ω.m (indicated in green). This medium-resistivity unit is underlain by an irregular, low-resistive layer, the upper boundary of which is outlined with a thick white dashed line, which depicts a bow-like geometry. It is not known what causes the low-resistivity layer.

The magnetic profile shown in Figure 10b indicates two high-magnetic anomalies, which are indicated by letters X and Y. The highest magnitude of anomaly X is about 50,000 nT, and its width is about 67 m. The second anomaly, labeled Y, has a magnitude of 49,500 nT, but its width is about 6 m. Both magnetic anomalies occur within the boundaries of volcanic rocks (tuff and lava).

Magnetic modeling of profile MR. A 2.5D magnetic modeling is one way to derive and/or evaluate subsurface geology (e.g.,

McLean and Betts, 2003), and it was implemented in this study. The magnetic data were acquired along five traverses (M1 through M4 and MR) across the area, but only one magnetic profile (MR) was associated with a resistivity profile (Figure 10). For this reason, magnetic profile MR was chosen for a 2.5D modeling exercise.

The initial geometry was based on a previously described geologic model and observed resistivity section, while assigned magnetic susceptibilities were within published values for the present rocks. The model did not account for the remnant magnetization due to lack of this information. Other parameters of the present-day magnetic field, such as magnetic inclination of 59° 1′ and declination of 4° 3′ were incorporated into the model (Figure 11).

During the modeling process, the initial geometries and magnetic susceptibilities were tuned to achieve a reasonable fit between observed and calculated magnetic response of the subsurface. Three magnetic zones were required along the magnetic profile MR to satisfy the observed anomaly: very high magnetization (red in color with a susceptibility of 0.264 SI), high magnetization (pink in color with a susceptibility of 0.126 SI), and low magnetization (light green with a susceptibility of 0.025 SI). The country rock limestone, indicated with a darker green, was assumed to have a zero SI unit susceptibility (Figure 11).

The interpretation of these magnetic zones is based on the surface observations and potential mechanism forming these geologic features (e.g., Griffin et al., 2005). Thus, the central part (in red) corresponds to the main magma feeder and the latest extrusion event, a lava infill of the central volcanic depression. The surrounding zone (pink) corresponds to undifferentiated interbedded volcanic tuffs and lavas. The low-magnetization zone (light green) was probably affected by intrusive and extrusive processes producing fracturing and brecciation of the country rock, small-scale igneous rock emplacements, and postintrusion percolation of fluids rich in magnetic minerals through this part of the section.

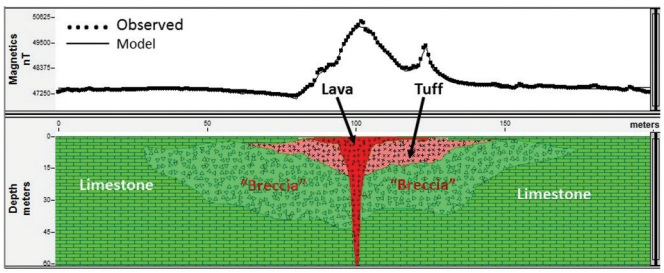

Figure 11. Forward model of magnetic profile MR. To have a good fit, very high (red), high (pink), and low (light green, breccia) magnetic zones were assumed. The magnetic susceptibility of the country rock (limestone) was taken zero (see text for detail). The width of the volcanic vent is about 17 m near the surface, but it decreases with depth.

Kiyosugi et al. (2012) define volcanic conduits as "plug-like" bodies in the San Rafael region of Utah, United States, as vertical intrusions >10 m in diameter in map view. The width of these volcanic plug bodies is <40 m. These observed parameters of diameter and width of eroded volcanic plugs are consistent with the dimensions of observed magnetic anomalies in this study.

3D northwest–southeast resistivity data. It should be pointed out that there is rapid variation in the resistivity anomalies from one profile to the profile discussed in the subsection on northwest-southeast resistivity data. This clearly means that the profiles contain anomalies that are generated by 3D objects, disrupted stratigraphy in the volcanic section, sizeable limestone blocks, and volcanic units (tuffs and lavas) with limited spatial extent.

For the reason mentioned above, pseudo-resistivity 3D block diagrams were constructed using 2D profiles of R1, R2, R3, R4, and R5 (Figure 12).

Figure 12a shows resistivity inversion parameters and indicates the good quality of the field data. Figure 12b displays a 3D resistivity map view of the study area, which indicates a well-defined low-resistivity anomaly bounded by the Vinson Chalk observed on the bed of Williamson Creek. Figure 12c provides a dynamic slice of the pseudo-3D diagram, which indicates the image of a volcanic vent (the two white lines).

2D and 3D northeast–southwest resistivity data. Figure 13 shows the resistivity data collected along three profiles (R6, R7, and R8; see Figure 6 for location). Urbanization in the study area did not allow longer extension of these profiles. A topographic correction for the creek was applied to each profile during processing of the resistivity data. The elevation data was obtained in the field using a tape measure. Volcanic rocks (lava and tuff) outcrop on the creek bed and on both sides of the creek banks, and their resistivity values range between approximately 3 and 20 Ω.m. However, this low-resistivity anomaly envelops blocks of higher-resistivity rocks in the middle of the profiles. Low-resistivity values extend under the terrace deposits on the southern creek bank and make contact with the higher resistivity values, which may be caused by Vinson Chalk. This boundary, shown by a thick black dashed line on resistivity profiles, could represent the volcanic vent's south termination. The thickness of the terrace deposits varies between 0.6 and 1 m.

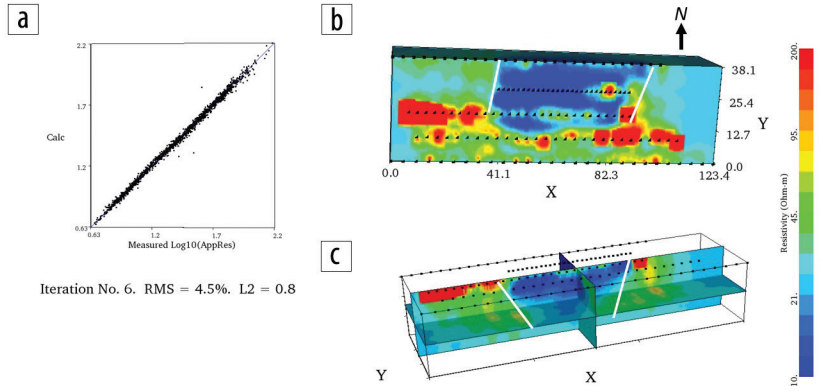

Figure 12. Pseudo-3D resistivity map. (a) Figure showing the inversion parameters; (b) and (c) display the map view and slice 3D diagrams across the geologic contacts of volcanic and limestone rock. View is from south to north. Geologic contacts between the volcanic rocks and the Vinson Chalk are depicted with a white line in (b) and (c).

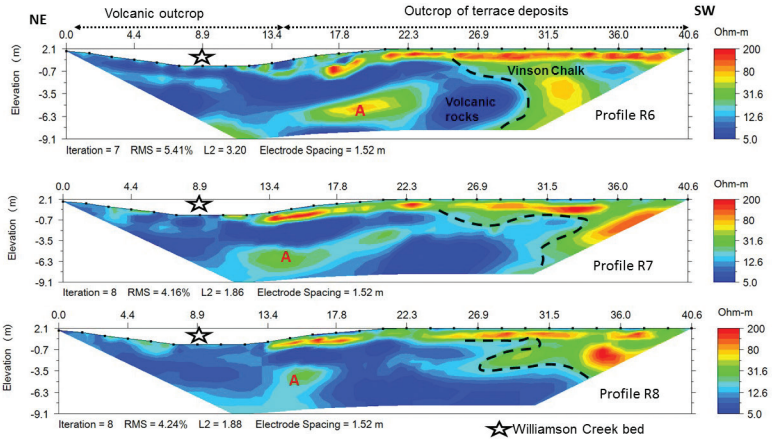

Figure 13. Resistivity data across Williamson Creek along profiles R6, R7, and R8. A black dashed line indicates the boundary between the volcanic and country rock (Vinson Chalk). Note the high-resistivity blocks (denoted by letter A) embedded within the volcanic rocks.

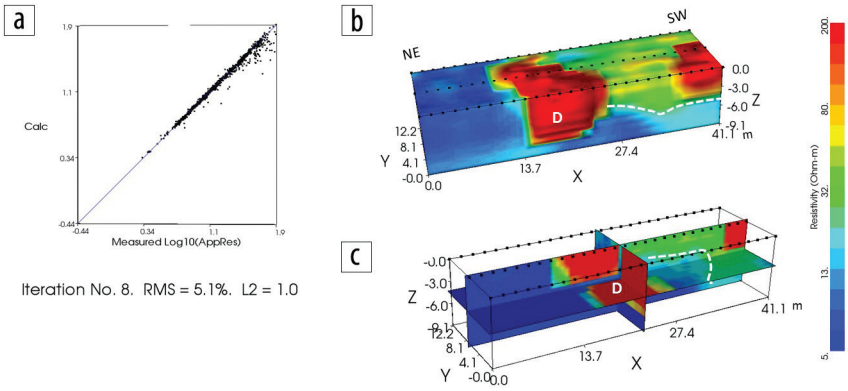

Figure 14. Pseudo 3D resistivity map: (a) shows the inversion parameters; (b) and (c) display the map and cross-section view and slice 3D diagrams. The dashed white line could be the geologic boundary between volcanic rocks and the Vinson Chalk. The high resistive anomaly (denoted by letter D) may correspond to the resistivity anomaly "A" in Figure 13.

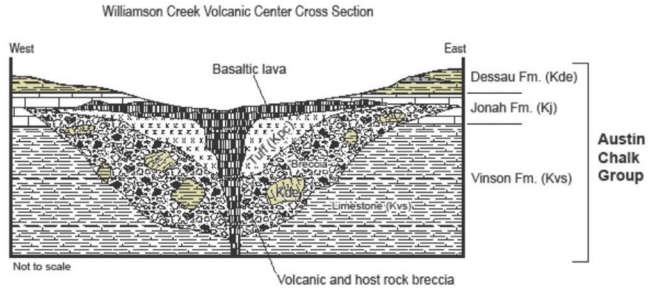

Figure 15. West-east geologic cross section of a volcanic vent based on geophysical (resistivity and magnetic) data, 2D modeling of magnetic data, and geologic data in the vicinity of the Williamson Creek (Young et al., 1982).

Pseudo-resistivity 3D block diagrams were constructed using three 2D north-south profiles (Figure 14). A topographic correction was not applied to the 3D data due to a limitation in the resistivity software. Figure 14a shows resistivity inversion parameters and indicates the good quality of the field data.

Figures 14b and 14c show both the map/side and slice views, which indicate a well-defined high-resistivity anomaly (red) in the center of the volcanic rocks. This anomaly is surrounded by low-resistivity values (blue and green) and is depicted with a letter D. The smaller, but similar, anomaly is also observed in the diagram's easternmost section. Both high-resistivity anomalies are probably caused by limestone blocks within the volcanic rocks.

Discussion and conclusions

The 2D and pseudo-3D resistivity results at the Williamson Creek site provide significant information on the lateral and vertical extent of the volcanic rocks and their structural status with the Vinson limestone of Austin Chalk Group. Two- and three-dimensional resistivity results indicate a low-resistivity anomaly bounded by a vent-like structure across the outcrop of the volcanic rocks.

The deepest resistivity (49 m) section along the south creek bank indicates flat low-resistivity units at shallow depths, but their bottom contacts with the underlying geologic unit are highly irregular. Furthermore, there are high-resistivity blocks scattered randomly below this contact that appear to cause the interfingering of volcanic rocks into the deeper section of the underlying geologic unit. These limestone blocks are probably erratic blocks of Vinson limestone or older Austin Chalk, which were probably torn from the walls of the volcanic vent and ejected. Numerous similar observations have been made over oil fields containing inclusions of fragments of Austin Chalk or older rocks within the volcanic eruption centers (Collingwood and Rettger, 1926; Simmons, 1967; Matthews, 1986). Beneath the exotic limestone blocks, there is a low-resistivity layer at the bottom of the resistivity profile, which is mapped along the entire length of the profile, and it shows an irregular geometry. It is not known what causes the low-resistivity layer.

Coincidence of the low-resistivity and the high-magnetic anomaly are strongly indicative of the igneous rock origin. Geometry of the 3D resistivity data appears to be associated with a steeply dipping funnel-shaped vent formation, which fed a volcanic edifice at the surface.

A schematic geologic cross section for the Williamson Creek site is created by integrating the resistivity and magnetic modeling results and the geologic map of the study area (Young et al., 1982) and is given in Figure 15. The section shows the volcanic vent rupturing through the Vinson and Jonah Formations of the Austin Group.

In summary, this geophysical study reveals that the lateral contacts between the volcanic rocks and the Vinson Chalk may not represent fault boundaries, but instead the walls of the magmatic intrusion associated with the onset of local volcanism. These

results indicate that the combination of resistivity and magnetic data may provide valuable information in delineating volcanic vents and dikes and defining the geologic contacts of volcanic rocks in the Austin area and in the state of Texas. Additional resistivity surveys, in conjunction with magnetic surveys, could offer useful information on the structure of volcanic plugs. The procedures developed here may have applications in other areas with comparable geologic conditions. TLE

Acknowledgments

I thank Chris Caran for introducing the site and his enthusiastic help in the field. I thank Brian Gieselman, Jeffrey Watson, Tyler Fritz, Jeffrey Pender, Alfred Hawkins, and Alan Cherepon for their help in the field. I also thank Vsevolod Egorov for his help on the modeling of the magnetic data. Special thanks are due to Michal Ruder, Darren Mortimer, Dave Smith, and Bruce Smith for reviewing the manuscript. I also greatly acknowledge Brian Hunt's contribution on the construction of the geologic section. Finally, I am grateful to Chuck Connor for his detailed and invaluable comments and revisions, which greatly improved this paper's content and flow.

Corresponding author: ega@pdq.net

References

Blaikie, T. N., L. Ailleres, R. A. F. Cas, and P. G. Betts, 2012, Three-dimensional potential field modelling of a multi-vent maar-diatreme — The Lake Coragulac maar, Newer Volcanics Province, south-eastern Australia: Journal of Volcanology and Geothermal Research, **235–236**, 70–83, http://dx.doi.org/10.1016/j.jvolgeores.2012.05.002.

Blaikie, T. N., L. Ailleres, P. G. Betts, and R. A. F. Cas, 2014, A geophysical comparison of the diatremes of simple and complex maar volcanoes, Newer Volcanics Province, south-eastern Australia: Journal of Volcanology and Geothermal Research, **276**, 64–81, http://dx.doi.org/10.1016/j.jvolgeores.2014.03.001.

Burke, W. H., J. B. Otto, and R. E. Denison, 1969, Potassium-argon dating of basaltic rocks: Journal of Geophysical Research, **74**, no. 4, 1082–1086, http://dx.doi.org/10.1029/JB074i004p01082.

Caran, C.S., T. Housh, A. Cherepon A, 2012, Volcanic features of the Austin area, Texas, Austin Geological Society Field Trip Guidebook 26.

Collingwood, D. M., 1930, Magnetics and geology of Yoast Field, Bastrop County, Texas: AAPG Bulletin, **14**, no. 9, 1191–1197.

Collingwood, D. M., and R. E. Rettger, 1926, The Lytton Springs oil field, Caldwell County, Texas: AAPG Bulletin, **10**, no. 10, 953–975.

Connor, C. B., and S. K. Sandberg, 2001, Application of integrated geophysical techniques to characterize the Edwards Aquifer, Texas: Bulletin of the South Texas Geological Society, **41**, no. 7, 11–25.

Dahlin, T., 1996, 2D resistivity surveying for environmental and engineering applications: First Break, **14**, no. 1137, 275–284, http://dx.doi.org/10.3997/1365-2397.1996014.

Dahlin, T., and M. H. Loke, 1997, Quasi-3D resistivity imaging-mapping of three dimensional structures using two dimensional DC resistivity techniques. Proceedings of the 3rd Meeting of the Environmental and Engineering Geophysical Society. 143-146.

De Filippis, L., E. Anzalone, A. Billi, C. Faccenna, P. P. Poncia, and P. Sella, 2013, The origin and growth of a recently-active fissure ridge travertine over a seismic fault, Tivoli, Italy, http://host.uniroma3.it/docenti/faccenna/Publication_files/DeFilippise-tal.13.geomor.pdf.

Dobecki T., and S. Church, 2006, Geophysical applications to detect sinkholes and ground subsidence, *The Leading Edge*, 25, no. 3, 336–341, http://dx.doi.org/10.1190/1.2184102.

Ewing, T. E., and S. C. Caran, 1982, Late Cretaceous volcanism in south and central Texas, stratigraphic, structural and seismic model: GCAGS Transactions, **32**, 137–145.

George, O. A., J. McIlrath, A. Farrell, E. Gallant, S. Kinman, A. Marshall, C. McNiff, M. Njoroge, J. Wilson, C. B. Connor, L. J. Connor, and S. Kruse, 2015, High-Resolution Ground-Based Magnetic Survey of a Buried Volcano: Anomaly B, Amargosa Desert, NV: Statistics in Volconalogy, **1**, 1–23, http://dx.doi.org/10.5038/2163-338X.1.3.

Griffin, R., T. Ewing, S. Bergman, and M. I. Leybourne, 2005, Volcanic Rocks of the Balcones Igneous Province, Field Trip Guidebook, GSA South Central Section Meeting, San Antonio, Texas.

Griffin, W. R., K. A. Foland, R. J. Stern, and M. I. Leybourne, 2010, Geochronology of bimodal alkaline volcanism in the Balcones Igneous Province, Texas: Implications for Cretaceous intraplate magmatism in the Northern Gulf of Mexico magmatic zone: The Journal of Geology, **118**, no. 1, 1–21, http://dx.doi.org/10.1086/648532.

Griffiths, D. H., and J. Turnbull, 1985, A multi-electrode array for resistivity surveying: First Break, **3**, no. 7, 16–20, http://dx.doi.org/10.3997/1365-2397.1985013.

Kiyosugi, K., C. B. Connor, P. H. Wetmore, B. P. Ferwerda, A. M. Germa, L. J. Connor, and A. R. Hintz, 2012, Relationship between dike and volcanic conduit distribution in a highly eroded monogenetic volcanic field: San Rafael, Utah, USA: Geology, **40**, no. 8, 695–698, http://dx.doi.org/10.1130/G33074.1.

López Loera, H., J. J. Aranda-Gomez, J. A. Arzate, and R. S. Molina-Garza, 2008, Geophysical surveys of the Joya Honda Maar (Mexico) and surroundings; volcanic implications: Journal of Volcanology and Geothermal Research, **170**, no. 3–4, 135–152, http://dx.doi.org/10.1016/j.jvolgeores.2007.08.021.

Marshall, A., C. Connor, S. Kruse, R. Malservisi, J. Richardson, L. Courtland, L. Connor, J. Wilson, and M. Karegar, 2015, Subsurface structure of a maar-diatreme and associated tuff-ring from a high-resolution geophysical survey, Rattlesnake Crater, Arizona: Journal of Volcanology and Geothermal Research, **304**, 253–264, http://dx.doi.org/10.1016/j.jvolgeores.2015.09.006.

Matthews, T. F., 1986, The petroleum potential of "serpentine plugs" and associated rocks, Central and South Texas: Baylor Geological Studies: Bulletin, **44**.

McLean, M. A., and P. G. Betts, 2003, Geophysical constraints of shear zones and geometry of the Hiltaba Suite granites in the western Gawler Craton, Australia: Australian Journal of Earth Sciences, **50**, no. 4, 525–541, http://dx.doi.org/10.1046/j.1440-0952.2003.01010.x.

Mrlina, J., H. Kampf, C. Kroner, J. Mingram, M. Stebich, A. Brauer, W. H. Geissler, J. Kallmeyer, H. Matthes, and M. Seidl, 2009, Discovery of the first Quaternary maar in the Bohemian Massif, Central Europe, based on combined geophysical and geological surveys: Journal of Volcanology and Geothermal Research, **182**, no. 1–2, 97–112, http://dx.doi.org/10.1016/j.jvolgeores.2009.01.027.

Saribudak, M., N. Hauwert, A. Hawkins, 2013, Geophysical signatures of Barton Springs (Parthenia, Zenobia and Eliza) of the Edwards Aquifer, Austin, Texas: Sinkhole Conference 14 proceedings, Carbonite and Evaporites, Springer Publishing, http://dx.doi.org/10.1007/s13146-013-0155-4.

Saribudak, M., and C. Caran, 2015, Resistivity, magnetic data delineate volcanic tuff in Travis County, Texas: Oil and Gas Journal, 113, no. 10, 52–57.
Sellards, E. H., 1932, Oil fields in igneous rocks in coastal plain of Texas: The American Association of Petroleum Geologists Bulletin, **16**, 741–768.
Simmons, K., 1967, A primer on "serpentine plugs" in South Texas, South Texas Geological Bulletin, 7, no. 2, 5–17.
Skácelová, Z., R. Vladislav, J. Valenta, F. Hartvich, J. Sramek, M. Radon, R. Gazdova, L. Novakova, P. Kolinsky, and Z. Pecskay, 2010, Geophysical research on structure of partly eroded maar volcanoes: Miocene Hnojnice and Oligocene Rychnov volcanoes (northern Czech Republic): Journal of Geosciences (Prague), **55**, 333–345.
Spencer, A. B., 1969, Alkalic igneous rocks of the Balcones Province, Texas: Journal of Petrology, **10**, no. 2, 272–306, http://dx.doi.org/10.1093/petrology/10.2.272.
Udden, J. A., and H. P. Bybee, 1916, The Thrall oil field: University of Texas Bulletin, 1, no. 66.
Xia, J., G. Ludvigson, R. D. Miller, L. Mayer, and A. Haj, 2010, A Delineation of a volcanic ash body using electrical resistivity profiling: Journal of Geophysics and Engineering, **7**, no. 3, 267–276, http://dx.doi.org/10.1088/1742-2132/7/3/005.
Young, K. P., S. C. Caran, and T. E. Ewing, 1982, Cretaceous volcanism in the Austin area, Texas, Austin Geological Society Guidebook 4.
Young, K. P., and C. M. Woodruff, 1985, Austin Chalk in its type area-Stratigraphy and Structure, Austin Geological Society Guidebook 7.